Eur. Phys. J. B **4**, 485–498 (1998)

THE EUROPEAN PHYSICAL JOURNAL B

Optimization of alloy-analogy-based approaches to the infinite-dimensional Hubbard model

M. Potthoff[a], T. Herrmann, and W. Nolting

Institut für Physik, Humboldt-Universität zu Berlin, 10115 Berlin, Germany

Received: 24 November 1997 / Revised: 16 March 1998 / Accepted: 28 April 1998

Abstract. An analytical expression for the self-energy of the infinite-dimensional Hubbard model is proposed that interpolates between different exactly solvable limits. We profit by the combination of two recent approaches that are based on the alloy-analogy (Hubbard-III) solution: the modified alloy-analogy (MAA) which focuses on the strong-coupling regime, and the Edwards-Hertz approach (EHA) which correctly recovers the weak-coupling regime. Investigating the high-energy expansion of the EHA self-energy, it turns out that the EHA reproduces the first three exactly known moments of the spectral density only. This may be insufficient for the investigation of spontaneous magnetism. The analysis of the high-energy behavior of the CPA self-consistency equation allows for a new interpretation of the MAA: the MAA is the only (two-component) alloy-analogy that correctly takes into account the first four moments of the spectral density. For small U, however, the MAA does not reproduce Fermi-liquid properties. The defects of the MAA as well as of the EHA are avoided in the new approach. We discuss the prospects of the theory and present numerical results in comparison with essentially exact quantum Monte-Carlo data. The correct high-energy behavior of the self-energy is proved to be a decisive ingredient for a reliable description of spontaneous magnetism.

PACS. 71.10.Fd Lattice fermion models (Hubbard model, etc.) – 75.10.Lp Band and itinerant models

1 Introduction

A central problem in solid-state physics concerns interacting electrons on a lattice. In dealing with itinerant magnetism, heavy-fermion compounds or high-temperature superconductivity, for example, electron-correlation effects are of exceptional significance. Much insight into the fundamental role of electron correlations can be gained by studying the Hubbard model [1–3]. In spite of its apparent simplicity, an exact solution for the whole parameter range is not available up to now, and a completely satisfactory understanding of its properties has not yet been achieved.

A notable exception is the extreme case of the one-dimensional model. In particular, the exact solution for the ground state is known in $d = 1$ [4]. The opposite limit of high spatial dimensions d, which has been introduced by Metzner and Vollhardt [5], is likewise important. For $d = \infty$ there are considerable simplifications that are due to the momentum independence of the electronic self-energy [6]. However, the infinite-dimensional model still remains non-trivial. It is of special interest since its essential properties are expected to be comparable to those at low dimensions $d = 2, 3$. If an approximation scheme was available that is reliable for the entire range of the model parameters in $d = \infty$, this would provide a proper dynamical mean-field theory in any dimension $d > 1$ [7,8].

Quantum Monte-Carlo (QMC) [9–11] and exact diagonalization methods (ED) [12,13] can yield essentially exact results but also suffer from limitations: ED is restricted to a rather small number of orbitals, and thus a smooth density of states cannot be obtained. On the other hand, QMC yields its results for the discrete Matsubara energies or along the imaginary time axis. Therefore, it is difficult to access the low-temperature regime where statistical errors become important within the QMC method. Furthermore, to obtain dynamical quantities it becomes necessary to perform an analytical continuation to the real axis which constitutes an ill-conditioned numerical problem. For these reasons the development of analytical (but approximate) methods for the infinite-dimensional Hubbard model still remains necessary.

An analytical approach to the $d = \infty$ Hubbard model should be guided by rigorously solvable limiting cases. There are a number of exact results which impose strong necessary conditions on any approximation: (i) second-order perturbation theory around the Hartree-Fock solution [14] (SOPT-HF) or self-consistent SOPT [6,15] yields the correct self-energy in the weak-coupling regime. (ii) The exact low-energy (Fermi-liquid) properties of the self-energy and the Luttinger sum rule [16] in particular have

[a] e-mail: michael.potthoff@physik.hu-berlin.de

been analyzed in reference [6] for the $d = \infty$ case. (iii) The atomic limit of vanishing hopping $t = 0$ represents an extreme but important limit. The first non-trivial correction to the atomic limit can be obtained from a canonical transformation of the Hubbard model that has first been considered by Harris and Lange [17,18]. For $U \mapsto \infty$ the approach provides rigorous information on the centers of gravity as well as on the spectral weights of the lower and upper Hubbard bands. (iv) The high-energy behavior of the self-energy is determined by the moments of the spectral density which can be calculated independently. For any U the high-energy behavior is important for a qualitatively correct description of the charge-excitation peaks. For $U \mapsto \infty$ the first four moments are necessary to be consistent with the results of Harris and Lange [19]. (v) Finally, the Falicov-Kimball model (FKM) [20] can be considered as a special limit of the Hubbard model. It is obtained by formally introducing a spin-dependent hopping and allowing only one of the two spin species to be mobile. The $d = \infty$ FKM is exactly solvable as has first been shown by Brandt and Mielsch [21]. The self-energy is given by the Hubbard-III alloy-analogy (AA) solution [22].

It may be interesting to have a theory at one's disposal that for arbitrary fillings recovers the weak-coupling, the atomic and the FKM limit, that is able to reproduce the first four moments of the spectral density and thereby the exact strong-coupling results of Harris and Lange, and that allows to directly treat zero temperature and real energies. The construction of such an approach is the main purpose of the present paper. To make contact with the FKM, the approach will be based on the alloy-analogy solution. The AA represents an attractive approximation which is simple, self-consistent and non-perturbative. On the other hand, there are defects that show up in other limits and that have given rise to modifications of the conventional AA.

A mean-field theory has been constructed in references [23,24] which is conceptually similar to the AA but in contrast to the latter derivable from an explicit free-energy functional and thus thermodynamically consistent and of variational character. This approach as well as the AA itself, however, cannot reproduce the aforementioned weak- and strong-coupling limits. The weak-coupling behavior of the AA is corrected within the Edwards-Hertz approach (EHA) [25–28]. A drawback of the EHA and also of the AA, however, consists in the fact that the strong-coupling results of Harris and Lange cannot be recovered. A recently proposed modified alloy analogy (MAA) [29] improves upon the AA and ensures consistency with the results of Harris and Lange for $U \mapsto \infty$. On the other hand, the MAA is not able to reproduce the Fermi-liquid properties for small U.

Our study aims at a proper combination of the MAA and the EHA which keeps their advantages and avoids their defects. After the necessary theoretical preparations (Sect. 2), we derive a helpful alternative interpretation of the MAA in Section 3. Section 4 concerns the high-energy expansion of the EHA self-energy. The analysis of the MAA and the EHA is a necessary condition for the concise presentation of the combined theory in Section 5. Numerical results obtained within the new method will be discussed for the paramagetic phase and in particular with respect to ferromagnetism (Sect. 6) before we come to the conclusions in Section 7.

2 Preparations

Using standard notations, the Hubbard Hamiltonian reads:

$$H = \sum_{ij\sigma} (T_{ij} - \mu\delta_{ij})\, c^\dagger_{i\sigma} c_{j\sigma} + \frac{1}{2} U \sum_{i\sigma} n_{i\sigma} n_{i-\sigma}. \tag{1}$$

The limit $d \mapsto \infty$ has to be taken with the proper scaling of the hopping integral between nearest neighbors to ensure the model to remain non-trivial [5]. For a hypercubic lattice with coordination number $Z = 2d$ and hopping $T_{\langle ij\rangle} \equiv t = t^*/\sqrt{2Z}$ ($t^* = const$) we get a Gaussian for the (non-interacting) Bloch-density of states (BDOS) [5]:

$$\rho^{(B)}(E) = \frac{1}{t^*\sqrt{\pi}} e^{-(E/t^*)^2}. \tag{2}$$

A generalization of the $d = 3$ fcc lattice to infinite dimensions with $Z = 2d(d-1)$ results in a strongly asymmetric Bloch-density of states [30]:

$$\rho^{(B)}(E) = \frac{e^{-(1+\sqrt{2}E/t^*)/2}}{t^*\sqrt{\pi(1+\sqrt{2}E/t^*)}}, \tag{3}$$

where the hopping integral between nearest neighbors T_{ij} is positive and $t = t^*/\sqrt{Z}$ [31].

In infinite dimensions the self-energy $\Sigma_\sigma(E)$ is $\mathbf{k}$ independent or site-diagonal [6]. For a homogeneous phase, the on-site one-electron Green function thus depends on the lattice geometry *via* the BDOS only:

$$G_\sigma(E) = \int_{-\infty}^{\infty} \frac{\hbar\rho^{(B)}(z)}{E - (z-\mu) - \Sigma_\sigma(E)}\, dz. \tag{4}$$

Let us consider its high-energy expansion:

$$G_\sigma(E) = \hbar \sum_{m=0}^{\infty} \frac{M^{(m)}_\sigma}{E^{m+1}}\,. \tag{5}$$

The expansion coefficient are the moments

$$M^{(m)}_\sigma = \frac{1}{\hbar} \int_{-\infty}^{\infty} E^m A_\sigma(E)\, dE \tag{6}$$

of the spectral density $A_\sigma(E) = -\frac{1}{\pi}\mathrm{Im}\, G_\sigma(E+i0^+)$. They can be calculated exactly by making use of an alternative but equivalent representation:

$$M^{(m)}_\sigma = \langle [\mathcal{L}^m c_{i\sigma}, c^\dagger_{i\sigma}]_+ \rangle. \tag{7}$$

Here $\mathcal{L}\mathcal{O} = [\mathcal{O}, H]_-$ denotes the commutator of an operator $\mathcal{O}$ with the Hamiltonian, and $[\cdots,\cdots]_+$ is the anticommutator. The calculation along equation (7) is straightforward. However, with increasing order m the moments include equal-time correlation functions of higher and higher order which have to be expressed by some means in terms of known quantities again. This fact limits the number of moments that can be used in practice. For the Hubbard model the moments are useful up to $m = 3$ (see Refs. [32,33], for example). In particular, we obtain for $d = \infty$:

$$\begin{aligned}
M_\sigma^{(0)} &= 1,\\
M_\sigma^{(1)} &= \widetilde{T}_0 + Un_{-\sigma},\\
M_\sigma^{(2)} &= \sum_j \widetilde{T}_{ij}\widetilde{T}_{ji} + 2\widetilde{T}_0 Un_{-\sigma} + U^2 n_{-\sigma},\\
M_\sigma^{(3)} &= \sum_{jk} \widetilde{T}_{ij}\widetilde{T}_{jk}\widetilde{T}_{ki}\\
&\quad + 3Un_{-\sigma}\sum_j \widetilde{T}_{ij}\widetilde{T}_{ji} + \widetilde{T}_0 U^2 n_{-\sigma}(2+n_{-\sigma})\\
&\quad + U^3 n_{-\sigma} + U^2 n_{-\sigma}(1-n_{-\sigma})\widetilde{B}_{-\sigma}. \qquad (8)
\end{aligned}$$

For abbreviation we have defined: $\widetilde{T}_{ij} = T_{ij} - \mu\delta_{ij}$, $\widetilde{T}_0 = \widetilde{T}_{ii}$ and $\widetilde{B}_\sigma = B_\sigma - \mu$. This so-called "band-shift" consists of higher-order correlation functions,

$$B_\sigma = T_0 + \frac{1}{n_\sigma(1-n_\sigma)}\sum_{j\neq i} T_{ij}\langle c_{i\sigma}^\dagger c_{j\sigma}(2n_{i-\sigma}-1)\rangle, \qquad (9)$$

but can be expressed in terms of the one-particle Green function [33]. Note that while the hopping T_{ij} as well as the correlation functions $\langle c_{i\sigma}^\dagger c_{j\sigma}(2n_{i-\sigma}-1)\rangle$ scale as $1/\sqrt{d}$ for $d \mapsto \infty$, the lattice sum in (9) remains finite. Contrary to the finite-dimensional case, however, the band-shift is $\mathbf{k}$ independent for $d = \infty$.

The coefficients in the $1/E$ expansion of the self-energy,

$$\Sigma_\sigma(E) = \sum_{m=0}^{\infty} \frac{C_\sigma^{(m)}}{E^m}, \qquad (10)$$

are obtained by inserting equations (5, 10) into (4) and taking the moments of the BDOS from (8) for $U = 0$:

$$\begin{aligned}
C_\sigma^{(0)} &= Un_{-\sigma},\\
C_\sigma^{(1)} &= U^2 n_{-\sigma}(1-n_{-\sigma}),\\
C_\sigma^{(2)} &= U^2 n_{-\sigma}(1-n_{-\sigma})\left(\widetilde{B}_{-\sigma} + U(1-n_{-\sigma})\right). \qquad (11)
\end{aligned}$$

Let us mention some available rigorous results for the weak- and the strong-coupling regime. For $U \mapsto \infty$ the spectrum is dominated by the two charge-excitation peaks (Hubbard bands). At each $\mathbf{k}$ point the centers of gravity as well as the spectral weights of the lower and the upper Hubbard band can be calculated exactly within a perturbational approach due to Harris and Lange [17,18] which uses t/U as an expansion parameter. For $d = \infty$ we have:

$$\begin{aligned}
T_{1\sigma}^{(HL)}(\mathbf{k}) &= (1-n_{-\sigma})\epsilon(\mathbf{k}) + n_{-\sigma}B_{-\sigma} + \mathcal{O}(t/U),\\
T_{2\sigma}^{(HL)}(\mathbf{k}) &= U + n_{-\sigma}\epsilon(\mathbf{k}) + (1-n_{-\sigma})B_{-\sigma} + \mathcal{O}(t/U),\\
\alpha_{1\sigma}^{(HL)}(\mathbf{k}) &= 1 - \alpha_{2\sigma}^{(HL)}(\mathbf{k}) = 1 - n_{-\sigma} + \mathcal{O}(t/U). \qquad (12)
\end{aligned}$$

The only difference to the finite-dimensional case [17] consists in the fact that the $\mathbf{k}$ dependence of the centers of gravity $T_{p\sigma}^{(HL)}(\mathbf{k})$ and the weights $\alpha_{p\sigma}^{(HL)}(\mathbf{k})$ $(p = 1, 2)$ is exclusively due to the Bloch dispersion $\epsilon(\mathbf{k})$. For finite d an additional $\mathbf{k}$ dependence is introduced *via* the band shift.

In the weak-coupling regime the usual perturbative approach applies. Up to order U^2 the self-energy is given by:

$$\Sigma_\sigma^{(SOPT)}(E) = Un_{-\sigma} + \Sigma_\sigma^{(SOC)}(E). \qquad (13)$$

The first-order term is the Hartree-Fock self-energy; the second-order contribution reads:

$$\begin{aligned}
\Sigma_\sigma^{(SOC)}(E) = \frac{U^2}{\hbar^3}\int\int\int \frac{A_\sigma^{(1)}(x)A_{-\sigma}^{(1)}(y)A_{-\sigma}^{(1)}(z)}{E-x+y-z}\\
\times(f(x)f(-y)f(z)\\
+f(-x)f(y)f(-z))\,dx\,dy\,dz. \qquad (14)
\end{aligned}$$

Here $f(x)$ is the Fermi function, and $A_\sigma^{(1)}(E)$ is defined as the free $(U = 0)$ spectral density shifted in energy by a (possibly spin-dependent) constant E_σ:

$$A_\sigma^{(1)}(E) = A_\sigma^{(0)}(E - E_\sigma). \qquad (15)$$

The shifts E_σ are introduced for later use. With $E_\sigma = 0$ the plain or conventional second-order perturbation theory (SOPT) and with $E_\sigma = Un_{-\sigma}$ the SOPT around the Hartree-Fock solution [14] is recovered. Both versions of SOPT as well as the self-consistent SOPT [6] are identical up to order U^2.

3 Modified alloy-analogy

The original alloy-analogy solution (AA) by Hubbard [22] is at variance with both, the exact weak- and strong-coupling results. Recently, a modified alloy-analogy solution (MAA) has been proposed [29] to overcome the drawbacks of the conventional AA with respect to the limit $U \mapsto \infty$. Any two-component alloy analogy requires the specification of the two atomic levels and the corresponding concentrations. The self-energy is then obtained from the CPA equation [34]:

$$0 = \sum_{p=1}^{2} x_{p\sigma}\,\frac{E_{p\sigma} - \Sigma_\sigma(E) - T_0}{1 - \frac{1}{\hbar}G_\sigma(E)\,[E_{p\sigma} - \Sigma_\sigma(E) - T_0]}\,. \qquad (16)$$

Within the conventional AA the levels and weights are taken from the atomic-limit solution [1], *i.e.*: $E_{1\sigma}^{(AA)} = T_0, E_{2\sigma}^{(AA)} = T_0 + U$ and $x_{1\sigma}^{(AA)} = 1 - n_{-\sigma}, x_{2\sigma}^{(AA)} = n_{-\sigma}$.

This choice, however, is by no means predetermined. Within the MAA [29] the self-energy $\Sigma_\sigma^{(MAA)}(E)$ is still obtained from the CPA equation (16), but the atomic levels and the concentrations are replaced by:

$$E_{p\sigma}^{(MAA)} = \frac{1}{2}\left(T_0 + U + B_{-\sigma}\right) + (-1)^p \times \sqrt{\frac{1}{4}\left(U + B_{-\sigma} - T_0\right)^2 + U n_{-\sigma}\left(T_0 - B_{-\sigma}\right)}, \quad (17)$$

and

$$x_{1\sigma}^{(MAA)} = \frac{B_{-\sigma} + U(1-n_{-\sigma}) - E_{1\sigma}^{(MAA)}}{E_{2\sigma}^{(MAA)} - E_{1\sigma}^{(MAA)}} = 1 - x_{2\sigma}^{(MAA)}. \quad (18)$$

The expressions include the band shift $B_{-\sigma}$. If $B_{-\sigma}$ is replaced by T_0, the MAA reduces to the conventional AA. As can be seen from equation (9) this replacement is correct for the atomic and for the "FKM limit". Furthermore, $B_{-\sigma} = T_0$ is required by particle-hole symmetry in the case of a paramagnet at half-filling. In all other cases the MAA is different from the AA. In particular, *via* the band shift the atomic levels might now become spin-dependent.

In the original work [29] the MAA has been derived by referring to the spectral-density approach (SDA) [32,33,35]. Considering the so-called split-band regime of the CPA [34], the consistency of the MAA with the results of Harris and Lange (12) could be proven for $U \mapsto \infty$.

For later purposes it is important to give another interpretation of the MAA which is different from the original one in reference [29]: since the atomic values and the concentrations that are needed to construct an alloy analogy for the Hubbard model are not predetermined, one can ask for the optimal choice (in some sense). In the following we argue that the MAA is obtained if one demands that the resulting theory should correctly take into account the first four moments of the spectral density given in equation (8).

We consider the CPA equation (16) as an equation for the self-energy that contains four unknown parameters, $E_{p\sigma}$ and $x_{p\sigma}$ $(p = 1, 2)$, which have to be fixed by imposing the correct results for the moments of the spectral density. Since the moments are closely related to the high-energy behavior of the Green function, we have to expand the CPA equation in powers of $1/E$ using equations (5, 10). Considering terms up to $1/E^2$, this yields the following equations:

$$\begin{aligned} 1 &= \sum_p x_{p\sigma}, \\ 0 &= \sum_p x_{p\sigma}\left(E_{p\sigma} - T_0 - C_\sigma^{(0)}\right), \\ 0 &= \sum_p x_{p\sigma}\left[(E_{p\sigma} - T_0 - C_\sigma^{(0)})^2 M_\sigma^{(0)} - C_\sigma^{(1)}\right], \\ 0 &= \sum_p x_{p\sigma}\left[(E_{p\sigma} - T_0 - C_\sigma^{(0)})^3 (M_\sigma^{(0)})^2 \right. \\ &\quad + (E_{p\sigma} - T_0 - C_\sigma^{(0)})^2 M_\sigma^{(1)} \\ &\quad \left. - 2(E_{p\sigma} - T_0 - C_\sigma^{(0)}) C_\sigma^{(1)} M_\sigma^{(0)} - C_\sigma^{(2)}\right]. \end{aligned} \quad (19)$$

Inserting the exact expansion coefficients (8, 11) for the Green function and for the self-energy and solving for $E_{p\sigma}$ and $x_{p\sigma}$, indeed yields the MAA results (17, 18).

This proves that the MAA not only recovers the exact strong-coupling results of Harris and Lange, but also (for arbitrary U) respects the conditions that are imposed on the overall shape of the spectral density by their exactly known first four moments. In this sense the MAA can be termed to be an optimal alloy analogy.

It is not very difficult to analyze the high-energy behavior of the conventional AA. Starting from equation (19) and inserting the AA levels and concentrations, it shows up that the last equation cannot be satisfied. While the AA yields the correct coefficients up to order $1/E$ in the expansion of the self-energy, it turns out that the coefficient $C_\sigma^{(2)}$ is not recovered. Instead, one gets: $C_\sigma^{(2,AA)} = C_\sigma^{(2)}|_{B_{-\sigma}\mapsto T_0}$. This is only exact in the atomic limit. Equivalently, it can be stated that the AA recovers three (instead of four) moments of the spectral density only.

While the MAA (in the sense of Harris and Lange) is correct in the strong-correlation regime, there is a severe drawback of the method: it fails to reproduce the Fermi-liquid properties for small interactions U. The same defect is inherent in the conventional AA.

4 Edwards-Hertz approximation

A correction of the conventional AA with respect to Luttinger's requirements and Fermi-liquid properties is due to Edwards and Hertz [25]. Just as the MAA improves upon the strong-coupling regime of the AA, the Edwards-Hertz approximation (EHA) corrects the AA in the weak-coupling regime.

The self-energy within the Edwards-Hertz approximation (EHA) is implicitly given by [25] (see also Refs. [26,27]):

$$\Sigma_\sigma^{(EHA)}(E) = \frac{U n_{-\sigma}}{1 - \frac{1}{\hbar}\widetilde{G}_\sigma(E)\left(U - \Sigma_\sigma^{(EHA)}(E)\right)}. \quad (20)$$

This equation is formally equivalent to the CPA equation (16) provided that the atomic levels and the concentrations are taken to be those of the conventional AA. Contrary to the AA, however, the one-particle Green function that occurs in the CPA equation, $G_\sigma(E)$, has been replaced by:

$$\widetilde{G}_\sigma(E) = \frac{\hbar}{U^2 n_{-\sigma}(1-n_{-\sigma})}\Sigma_\sigma^{(SOC)}(E - \Sigma_\sigma^{(EHA)}(E) + E_\sigma). \quad (21)$$

$\Sigma_\sigma^{(SOC)}(E)$ is the second-order contribution to the SOPT self-energy introduced in equation (14). The replacement is more or less ad hoc to enforce the correct weak-coupling behavior of the theory.

The shifts E_σ that appear in the definition (15) of the spectral density $A_\sigma^{(1)}(E)$ and once more in equation (21) have been introduced by Wermbter and Czycholl [27]. They are necessary to ensure that the EHA is exact in the atomic limit for all band-fillings. The shifts have to be determined self-consistently by the following requirement:

$$\begin{aligned} n_\sigma &= \int_{-\infty}^{\infty} f(E)\, A_\sigma(E)\, dE \\ &= \int_{-\infty}^{\infty} f(E)\, A_\sigma^{(1)}(E)\, dE. \end{aligned} \tag{22}$$

The EHA should be regarded as an interpolation scheme. It yields the correct results in the atomic as well as in the FKM limit and is exact for small U up to order U^2 [27]. The latter implies that the expansion in U satisfies Luttinger's requirements. However, Fermi-liquid behavior breaks down in a parameter region where the series diverges [25].

Let us now investigate the high-energy behavior of the EHA self-energy:

$$\Sigma_\sigma^{(EHA)}(E) = \sum_{m=0}^{\infty} \frac{C_\sigma^{(m,EHA)}}{E^m}\,. \tag{23}$$

First, we need the high-energy expansion of the modified propagator $\widetilde{G}_\sigma(E)$. Applying the Kramers-Kronig relation, it can be written in the form:

$$\begin{aligned} \widetilde{G}_\sigma(E) = {} & \frac{\hbar}{U^2 n_{-\sigma}(1-n_{-\sigma})} \\ & \times \int \frac{-\frac{1}{\pi}\mathrm{Im}\,\Sigma_\sigma^{(SOC)}(E'+i0^+)}{E-\Sigma_\sigma^{(EHA)}(E)+E_\sigma-E'}\, dE'. \end{aligned} \tag{24}$$

When expanding in powers of $1/E$, the following relations are needed:

$$\begin{aligned} \int -\frac{1}{\pi}\mathrm{Im}\,\Sigma_\sigma^{(SOC)}(E+i0^+)\, dE &= U^2 n_{-\sigma}(1-n_{-\sigma}), \\ \int -\frac{1}{\pi}\mathrm{Im}\,\Sigma_\sigma^{(SOC)}(E+i0^+)\, E\, dE &= U^2 n_{-\sigma}(1-n_{-\sigma}) \\ & \times \left(B_{-\sigma}^{(1)} - \mu + E_\sigma\right). \end{aligned} \tag{25}$$

Using equation (22) these results can be derived from equation (14) immediately. For abbreviation we have defined:

$$B_\sigma^{(1)} = T_0 + \frac{2n_{-\sigma}-1}{n_\sigma(1-n_\sigma)} \sum_{j\neq i} \widetilde{T}_{ij} \langle c_{i\sigma}^\dagger c_{j\sigma}\rangle^{(1)}, \tag{26}$$

where the one-particle correlation function results from the free ($U=0$) but shifted off-diagonal Green function: $\langle c_{i\sigma}^\dagger c_{j\sigma}\rangle^{(1)} = -\frac{1}{\hbar\pi}\int f(E)\,\mathrm{Im}\,G_{ij\sigma}^{(0)}(E+i0^+-E_\sigma)dE$. The expansion of the modified propagator then reads:

$$\frac{1}{\hbar}\widetilde{G}_\sigma(E) = \frac{1}{E} + \left(B_{-\sigma}^{(1)} - \mu + U n_{-\sigma}\right)\frac{1}{E^2} + \cdots \tag{27}$$

The coefficients in this expansion are the moments of the (fictive) spectral density $\widetilde{A}_\sigma(E) \equiv -(1/\pi)\mathrm{Im}\,\widetilde{G}_\sigma(E+i0^+)$ (This will become important in the next section). Inserting the result and the ansatz (23) in equation (20) and grouping the terms in powers of $1/E$, we finally obtain:

$$\begin{aligned} C_\sigma^{(0,EHA)} &= U n_{-\sigma}, \\ C_\sigma^{(1,EHA)} &= U^2 n_{-\sigma}\,(1-n_{-\sigma})\,, \\ C_\sigma^{(2,EHA)} &= U^2 n_{-\sigma}\,(1-n_{-\sigma})\left(B_{-\sigma}^{(1)} - \mu + U(1-n_{-\sigma})\right). \end{aligned} \tag{28}$$

Comparing with equation (11), we notice that the first two coefficients $C_\sigma^{(0)}$ and $C_\sigma^{(1)}$ are predicted correctly. As in the conventional AA, however, the third expansion coefficient turns out to be wrong: $C_\sigma^{(2,EHA)} = C_\sigma^{(2)}|_{B_{-\sigma}\mapsto B_{-\sigma}^{(1)}}$. Again, the replacement $B_{-\sigma} \mapsto B_{-\sigma}^{(1)}$ is correct in the atomic limit only. Furthermore, *via* equations (4, 5, 10) we can conclude that the fourth moment of the spectral density, $M_\sigma^{(3)}$, is not recovered within the EHA. Finally, this implies that for $U \mapsto \infty$ the EHA is at variance with the exact results of Harris and Lange (Eq. (12)).

5 Combining the approaches

We are now in a position to profit from the preceding analysis of the MAA and the EHA. We like to tackle the question whether a proper combination of both approaches is able to avoid their respective defects and to keep their advantages.

The following simple idea suggests itself: we start from the general CPA equation (16), replace the one-particle Green function $G_\sigma(E)$ by the modified propagator $\widetilde{G}_\sigma(E)$ as in the EHA, but take the atomic levels $E_{p\sigma}$ and the weights $x_{p\sigma}$ from the MAA according to equations (17, 18). It can be shown, however, that such an ansatz is neither correct up to order U^2 nor it recovers the high-energy coefficients up to order $1/E^2$.

We thus have to disregard the MAA levels and weights, but can try to retain the basic concept of the approach. In Section 4 we have interpreted the MAA as being the only (two-component) alloy analogy that correctly takes into account the first four moments of the spectral density: insisting on the correctness of the moments, unambiguously determines the levels and weights that appear in the CPA equation. Therefore, if we change the CPA equation by introducing the modified propagator $\widetilde{G}_\sigma(E)$, we must allow the parameters to adjust in order to keep the moments correct. This concept turns out to be successful indeed. For clarity in the notations let us refer to this approach as an "interpolating alloy-analogy-based"

approximation (IAA) since we can show that it recovers the weak-coupling limit and satisfies the requirements of Harris and Lange for strong U.

To begin with, we once more consider equation (16) with $G_\sigma(E)$ replaced by $\widetilde{G}_\sigma(E)$ and with *a priori* unknown parameters $E_{p\sigma}$ and $x_{p\sigma}$. As in the EHA the modified propagator $\widetilde{G}_\sigma(E)$ is defined by equation (21). To make contact with the moments of the spectral density, we have to expand the equation in powers of $1/E$. This yields equation (19) where the quantities $M_\sigma^{(m)}$ now have to be interpreted as the moments of the modified propagator $\widetilde{G}_\sigma(E)$. Fortunately, only the first two moments are needed which can be taken from equation (27). To ensure the correctness of the moments (8) within the IAA, we then have to insert the exact expressions (11) for the coefficients $C_\sigma^{(m)}$, which yields the following system of equations:

$$\begin{aligned}
&\sum_p x_{p\sigma}^{(IAA)} = 1\\
&\sum_p x_{p\sigma}^{(IAA)}\,(E_{p\sigma}^{(IAA)} - T_0) = Un_{-\sigma},\\
&\sum_p x_{p\sigma}^{(IAA)}\,(E_{p\sigma}^{(IAA)} - T_0)^2 = U^2 n_{-\sigma},\\
&\sum_p x_{p\sigma}^{(IAA)}\,(E_{p\sigma}^{(IAA)} - T_0)^3 = U^3 n_{-\sigma}\\
&+U^2 n_{-\sigma}(1-n_{-\sigma})\left(B_{-\sigma} - B_{-\sigma}^{(1)}\right). \qquad (29)
\end{aligned}$$

Solving for $E_{p\sigma}^{(IAA)}$ and $x_{p\sigma}^{(IAA)}$, we obtain:

$$E_{p\sigma}^{(IAA)} = T_0 + \frac{1}{2}\left(U + B_{-\sigma} - B_{-\sigma}^{(1)}\right) + (-1)^p \times \sqrt{\frac{1}{4}\left(U + B_{-\sigma} - B_{-\sigma}^{(1)}\right)^2 + Un_{-\sigma}\left(B_{-\sigma}^{(1)} - B_{-\sigma}\right)}, \qquad (30)$$

and

$$\begin{aligned}
x_{1\sigma}^{(IAA)} &= \frac{B_{-\sigma} - B_{-\sigma}^{(1)} + T_0 + U(1-n_{-\sigma}) - E_{1\sigma}^{(IAA)}}{E_{2\sigma}^{(IAA)} - E_{1\sigma}^{(IAA)}}\\
&= 1 - x_{2\sigma}^{(IAA)}. \qquad (31)
\end{aligned}$$

The results turn out to represent a slight modification of the corresponding MAA results which are obtained if $B_{-\sigma}^{(1)}$ is (*ad hoc*) replaced by T_0. In the last section we have recognized that the more simple one-particle correlation functions $B_{-\sigma}^{(1)}$ instead of the higher-order correlations $B_{-\sigma}$ appear in the expansion coefficient $C_\sigma^{(2,EHA)}$ of the EHA. Thus, it can be well understood that the difference $B_{-\sigma} - B_{-\sigma}^{(1)}$ is contained in (30, 31). If the difference is neglected, we will get the atomic levels and weights of the conventional AA again.

This concludes the theory. However, we still have to check whether the IAA self-energy is correct up to order U^2. This is by no means obvious since the U dependence of the atomic levels and the weights has become more complicated. Using the results (30, 31) in the CPA equation (16), we obtain for the IAA self-energy:

$$\Sigma_\sigma^{(IAA)}(E) = \frac{Un_{-\sigma}}{1 - \dfrac{(1/\hbar)\widetilde{G}_\sigma(E)\left(U - \Sigma_\sigma^{(IAA)}(E)\right)}{1 - (1/\hbar)\widetilde{G}_\sigma(E)\left(B_{-\sigma} - B_{-\sigma}^{(1)}\right)}}. \qquad (32)$$

The expression clearly shows the differences with respect to the conventional AA as well as to the EHA. The equation can be expanded in powers of U up to U^2 without knowing about the explicit U dependence of the modified propagator. However, we need:

$$B_{-\sigma} - B_{-\sigma}^{(1)} = const \times U + \mathcal{O}(U^2), \qquad (33)$$

which can be verified easily [19]. Using (33), it turns out that up to order U^2 we have:

$$\Sigma_\sigma^{(IAA)}(E) = Un_{-\sigma} + U^2 n_{-\sigma}(1-n_{-\sigma})\frac{1}{\hbar}\widetilde{G}_\sigma(E), \qquad (34)$$

which is the same result as found in the EHA and thus proves the IAA to be exact up to order U^2 indeed (*cf.* Ref. [27]):

$$\Sigma_\sigma^{(IAA)}(E) = Un_{-\sigma} + \Sigma_\sigma^{(SOC)}(E) + \mathcal{O}(U^3). \qquad (35)$$

Let us briefly check the other limiting cases mentioned: it goes without saying that the trivial cases of $U = 0$, $n = 0$ or $n = 2$ as well as the requirements imposed by particle-hole symmetry and the Herglotz properties [36] are fulfilled. Suppressing the hopping of the $\downarrow$-electrons, we have $B_\uparrow = B_\uparrow^{(1)} = T_0$ from equations (9, 26). Hence, the theory reduces to the EHA and is thereby [27] correct for the Falicov-Kimball model and also in the atomic limit. By construction, the IAA self-energy has the correct high-energy expansion coefficients up to order $1/E^2$, and thus the moments of the spectral density $M_\sigma^{(0)}$ up to $M_\sigma^{(3)}$ are reproduced exactly. It can be shown analytically (similar to the discussion in Ref. [19]) or can simply be taken from the results presented in the next section that for strong U the **k**-resolved spectral density for each **k**-point consists of two dominant peaks (Hubbard bands). Their energetic distance is roughly given by U. Since the first four moments of the spectral density are also conserved for each **k**-point separately [37], the centers of gravity as well as the weights of both, the lower and the upper Hubbard band, are fixed and can be calculated analytically for $U \mapsto \infty$ along the lines of reference [32], for example. The result turns out to be identical to what has been derived within the t/U-perturbation theory of Harris and Lange (see Eq. (12)). Concludingly, the IAA improves upon the MAA with respect to the weak-coupling and upon the EHA what concerns the strong-coupling regime.

6 Discussion and results

6.1 Paramagnetic phase

For the symmetric case of half-filling and paramagnetism, electron-hole symmetry requires $B_\sigma = B_\sigma^{(1)} = T_0$.

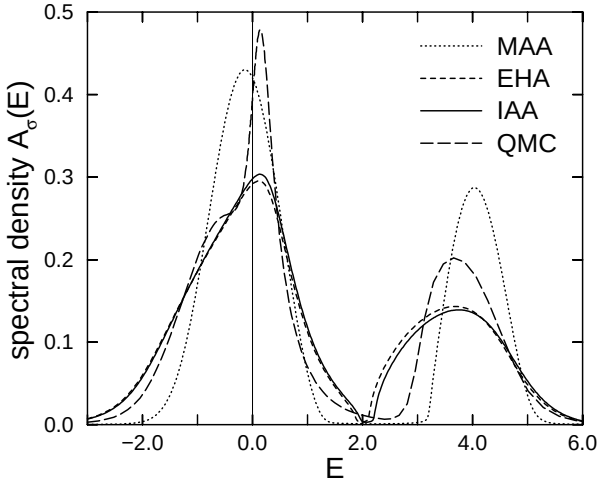

Fig. 1. Spectral density of the Hubbard model on the $d = \infty$ hyper-cubic lattice for on-site Coulomb interaction $U = 4$, band-filling $n = 0.79$ and inverse temperature $\beta = 7.2$. Results for the modified alloy-analogy (MAA), the Edwards-Hertz approach (EHA) and the interpolating alloy-analogy-based approximation (IAA) in comparison with quantum Monte-Carlo data (QMC) from Jarrell and Pruschke [38]. All energies are given in units of $t^* = 1$.

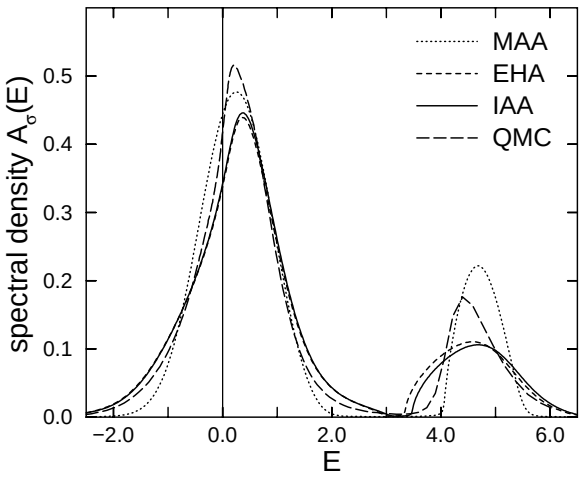

Fig. 2. The same as Figure 1, but for smaller band-filling $n = 0.57$.

This implies that the IAA reduces to the EHA in this case and thus cannot contribute to an improved description of the Mott transition. We therefore focus on the non-symmetric case $n \neq 1$. Figure 1 shows the spectral density of the $d = \infty$ Hubbard model on the hyper-cubic lattice for $U = 4$ and $n = 0.79$ as resulting from the MAA, the EHA and the IAA (units are chosen such that $t^* = 1$). A non-zero temperature has been taken ($\beta = 1/k_B T = 7.2$) to enable a direct comparison with the essentially exact QMC result of Jarrell and Pruschke [38] which is also shown in the figure.

For each of the three approximate theories, the spectrum mainly consists of the two dominant charge-excitation peaks (Hubbard bands). Compared with the MAA result, we notice that both peaks are significantly broadened within the IAA, their spectral weights being almost unchanged. Furthermore, while the MAA predicts nearly symmetric peak shapes, a clear peak asymmetry is observed within the IAA spectrum. The broadening effect can partly be traced back to a stronger quasi-particle damping in the IAA compared with the MAA: the imaginary part of the IAA self-energy is significantly larger at the energetic positions of the Hubbard bands.

The IAA spectrum is found to be only slightly different from the EHA result: comparing with the EHA, we find the IAA spectral density to be somewhat larger at its peak maximum in the lower Hubbard band. There is more weight in the lower and less weight in the upper peak which is shifted to higher energies compared with the EHA.

Besides the high-energy charge excitation peaks, the spectrum obtained by QMC simulations [38] shows up a third structure around the Fermi edge at $E = 0$, which is reminiscent of the Kondo resonance. In the present situation, away from half-filling and for finite temperature, the resonance is strongly broadened but still clearly visible. On the other hand, it is missing in the approximate approaches even for $T = 0$ and increased band-filling, although the correct trend can be recognized in the asymmetry of the IAA (and EHA) lower peak. Compared with the QMC result, the MAA predicts a too large (quasi) gap between the peaks, while it is too small within the IAA and EHA. The IAA (EHA) yields a width of the lower peak that is quite close to the QMC result. The width of the upper peak, however, comes out to large, while it is underestimated by the MAA. Passing from the EHA to the IAA, the agreement with the QMC result is improved very slightly.

Decreasing the band filling, we find the same qualitative differences between the approximate approaches. However, they become less pronounced. This can be seen in Figure 2 where the corresponding results are shown for $n = 0.57$. Comparing with the QMC spectrum, some discrepancies also remain for lower n, but the overall agreement is certainly improved for all approaches considered. This is mainly due to the fact that the Kondo-like resonance has disappeared in the QMC spectrum.

With respect to the EHA the main conceptual improvement of the IAA consists in the corrected high-energy behavior of the self-energy. This is determined by the correlation function $B_{-\sigma}$. In the strong-coupling regime $B_{-\sigma}$ leads to an effective shift of the lower Hubbard band $n_{-\sigma} B_{-\sigma}$ (*cf.* Eq. (12)). This is shown in Figure 3 as a function of n. For the IAA as well as for the MAA the overall dependence on n is quite similar to the results known from the spectral-density approach [29,35] as well as from the modified perturbation theory [19]. We notice that (within the IAA) there is a small difference between $B_{-\sigma}$ and its Hartree-Fock value $B^{(1)}_{-\sigma}$ only. Consequently, this implies *via* equations (20, 32) that

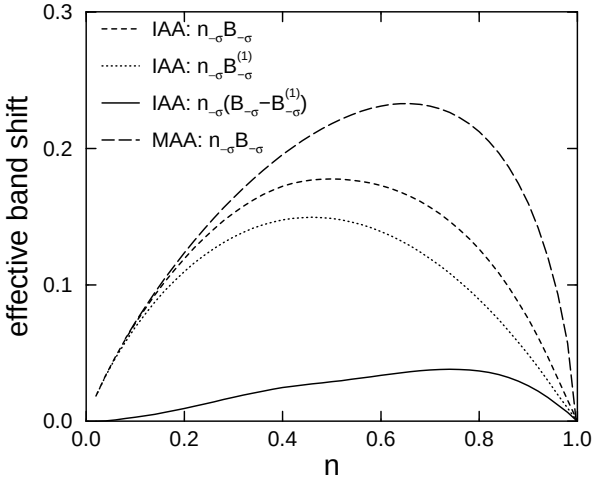

Fig. 3. Effective band shift $n_{-\sigma}B_{-\sigma}$ for the MAA and the IAA and $n_{-\sigma}B^{(1)}_{-\sigma}$ (Hartree-Fock value, IAA) as a function of band-filling n. Hyper-cubic lattice, $U = 4$, $\beta = 7.2$, $n_\uparrow = n_\downarrow$. Results are symmetric to the $n = 1$ axis.

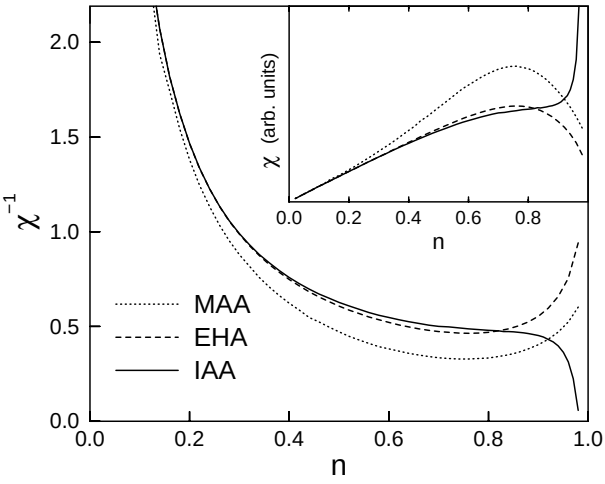

Fig. 4. Inverse static susceptibility χ^{-1} (inset: χ) as a function of band-filling n for the hyper-cubic lattice, $U = 4$ and $\beta = 7.2$. Results for the MAA, EHA and IAA.

for the IAA only minor changes can be expected with respect to the EHA. This is consistent with the results for the spectral density discussed above.

6.2 Ferromagnetism

Within the self-consistent calculation, the correlation functions $B_{-\sigma}$ might become spin-dependent. According to equation (12) this would imply a spin-dependent shift of the centers of gravity of the two Hubbard bands. Therefore, the band shift $B_{-\sigma}$ is of exceptional importance for the possibility and thermodynamical stability of spontaneous ferromagnetic order.

We consider two different cases where essentially exact QMC results are available: the hyper-cubic lattice with the BDOS given by equation (2), and the BDOS (3) corresponding to an fcc-type lattice. A ferromagnetic instability is indicated by a divergency of the uniform static susceptibility which is calculated within the paramagnetic phase in the limit of an infinitesimally small applied field H: $\chi \sim \partial(n_\uparrow - n_\downarrow)/\partial H|_{H=0}$. Jarrell and Pruschke [38] found a non-diverging susceptibility within QMC on the hyper-cubic lattice for various fillings and temperatures and interactions up to $U = 8$. This is consistent with the findings of references [39,40] where it is proved that the Nagaoka state [41] is instable for any $n \neq 1$. Let us mention, however, that a partially polarized ferromagnetic state has been found recently for $U \mapsto \infty$ within the non-crossing approximation [42].

The QMC result for $U = 4$ and $\beta = 7.2$ shows χ to be a monotonically increasing function of the filling up to $n = 1$ with a slightly negative curvature, $\partial^2\chi/\partial n^2 < 0$ [38]. Figure 4 shows the corresponding results from our analytical approaches. First, we notice a zero of χ^{-1} at $n = 0.98$ within the IAA. A non-zero magnetization is found for $0.98 \leq n \leq 1.02$ indeed. However, this has not been analyzed in more detail since obviously (comparing with QMC) it has to be interpreted as an artefact of the method. All three approaches considered cannot be expected to yield reliable results near to half-filling: in this range antiferromagnetic spin fluctuations are known to become important which manifest themselves in a narrow Kondo-like resonance at the Fermi level. The resonance, however, was shown to be absent in the analytical approaches (see above).

Well below half-filling the IAA predicts a rather featureless positive susceptibility which increases with increasing n and shows up a negative curvature. All this agrees with the QMC result. It should be mentioned that there are only minor changes in the results for temperature $T \mapsto 0$. In particular, for the IAA we have checked that the artificial ferromagnetic solution is always confined to the very small range around half-filling. The differences with respect to the EHA result are again found to be small except for fillings close to $n = 1$ where the results are unphysical anyway. Finally, we notice that within the MAA the functional dependence of χ on n shows up the wrong curvature for smaller n and disagrees in this respect with the QMC as well as with the IAA result.

A non-bipartite lattice as well as a strongly asymmetric BDOS are known to favor ferromagnetic order. This has been demonstrated in a comprehensive way by recent QMC studies [43–45] and variational approaches [46]. The results of Uhrig [40] and Ulmke [44] show a ferromagnetic phase to be stable in a fairly extended region of the U-n-T phase diagram for the $d = \infty$ fcc-type lattice. Ferromagnetism is favored due to the strong asymmetry of the BDOS (3) with its square-root divergency at the lower band edge.

Thermodynamically stable ferromagnetic solutions are found within the MAA, the EHA as well as in the IAA. Figure 5 shows the temperature dependence of the spontaneous magnetization $m = n_\uparrow - n_\downarrow$ for $U = 4$ ($t^* = 1$)

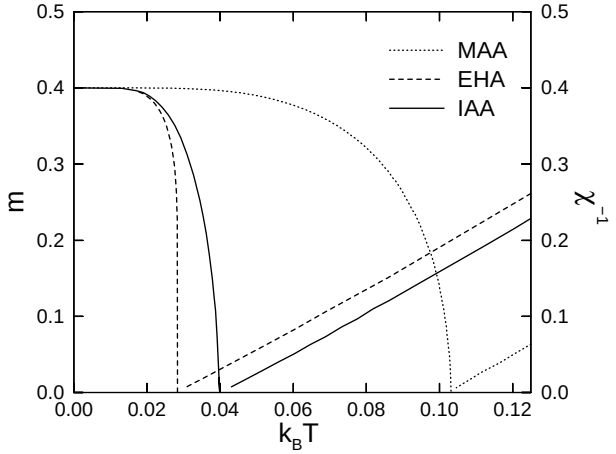

Fig. 5. Spontaneous magnetization $m = \langle n_\uparrow \rangle - \langle n_\downarrow \rangle$ and inverse static susceptibility χ^{-1} as functions of temperature for the Hubbard model on the $d = \infty$ fcc-type lattice (*cf.* BDOS in Eq. (3)) for $U = 4$ and $n = 0.4$. Results for the MAA, EHA and IAA.

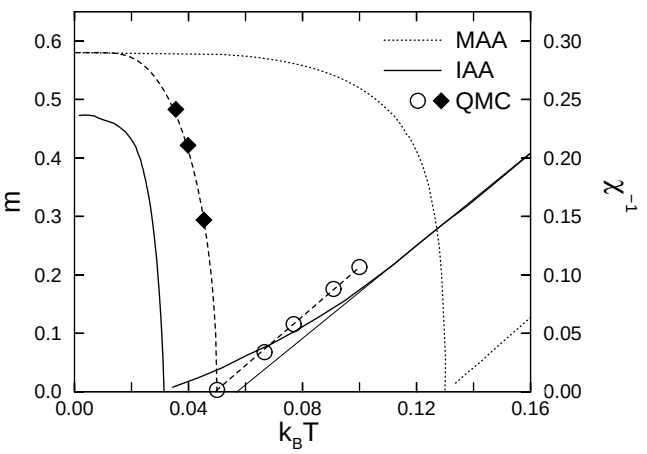

Fig. 6. Temperature dependence of m and χ^{-1} for $U = 4$ and $n = 0.58$. Results for the MAA and IAA in comparison with the quantum Monte-Carlo data (QMC) from Vollhardt *et al.* [43] (diamonds/circles, dashed line: linear fit to χ^{-1} / fit with a Brillouin function to m). The thin solid line is a linear extrapolation of (the IAA) $\chi^{-1}(T)$ to lower temperatures.

and $n = 0.4$. In each case a fully polarized state ($m = n$) is obtained for $T = 0$. Increasing the temperature results in a decrease of m. The magnetization curves are Brillouin-function-like, and the estimated critical exponent of the order parameter is $\beta = 1/2$, *i.e.* the expected mean-field value. The inverse susceptibility is also shown in Figure 5. At the respective Curie temperature T_C there is a zero of χ^{-1} as it must be for a second-order phase transition. For $T > T_C$ the temperature dependence of χ^{-1} is almost linear and thereby follows the Curie-Weiss law. For the critical exponent of the susceptibility we obtain the mean-field value $\gamma = 1$. The Curie temperature predicted by the IAA ($T_C = 0.040$) almost perfectly agrees with the essentially exact QMC result ($T_C = 0.039$ [44]).

For larger filling, at $n = 0.58$, QMC data [43,44] are available for the temperature dependence of m and χ^{-1}. The comparison with the MAA and IAA results is shown in Figure 6. In both cases a stable ferromagnetic solution and a second-order transition to the paramagnetic phase is found. For high temperatures the inverse static susceptibilities obey the Curie-Weiss law. As $T \to T_C$, however, the IAA inverse susceptibility deviates from the linear behavior. This is not observed for lower fillings (Fig. 5). The zero of χ^{-1} determines the Curie temperature $T_C = 0.031$ while the zero obtained from the extrapolation of the linear high-temperature trend yields the paramagnetic Curie temperature $\Theta = 0.057$. The correct (QMC) Curie temperature is found in between: $T_C = 0.05$ [43,44]; yet the agreement with respect to T_C is reasonable. However, the non-linear trend of $\chi^{-1}(T)$ near T_C is at variance with the QMC result. Also the $T = 0$ magnetization ($m = 0.47$) comes out too small since the Brillouin-function fit to the QMC data for m indicates a fully polarized ground state ($m = n = 0.58$).

The IAA results for $n = 0.58$ appear to be less reliable than those for $n = 0.4$. Still, the IAA turns out to be superior compared to the MAA, which yields a considerably too high Curie temperature ($T_C = 0.130$), and also to the EHA: at $n = 0.58$ the EHA does not yield a ferromagnetic solution at all, and we are left with the paramagnetic phase only.

In the discussion of the paramagnet, it has been mentioned that because of the absence of the Kondo-like feature in the IAA spectrum, reliable results cannot be expected for fillings close to half-filling. A restricted range of validity is also found with respect to the magnetic properties. The IAA is able to predict a reliable value for the Curie temperature for fillings up to $n \approx 0.5$ only. Below $n = 0.5$, however, the agreement between the IAA and QMC is convincing: Figure 7 shows the calculated filling dependence of T_C for $U = 4$. The phase transition is always of second order. For $n < 0.5$ the IAA result falls into the error bounds of the QMC data (except for $n = 0.2$). Possibly, there is a slight tendency to overestimate T_C in general. For $n > 0.5$ the Curie temperature steeply decreases with increasing filling. Beyond $n > 0.61$ only the paramagnetic solution can be found, while the ferromagnetic region extends up to $n \approx 0.88$ within QMC.

The MAA considerably overestimates the possibility for ferromagnetism. Over the whole n range considered, the Curie temperature is too large by more than a factor 2. Ferromagnetic solutions exist for $0 < n \lesssim 1$ (close to half-filling we encountered numerical difficulties to stabilize truly converged solutions). The $T_C(n)$ obtained by means of the EHA is similar to the IAA curve. As can be seen in Figure 7, however, T_C is too small compared with the QMC result if $n > 0.3$, and the ferromagnetic region shrinks to $n < 0.51$ in the EHA, thereby underestimating the possibility for ferromagnetic order. The IAA, being a combination of the MAA and the EHA, yields a T_C in between and the best agreement with the QMC result.

The interpretation for the different transition temperatures in the different approaches is the following: that

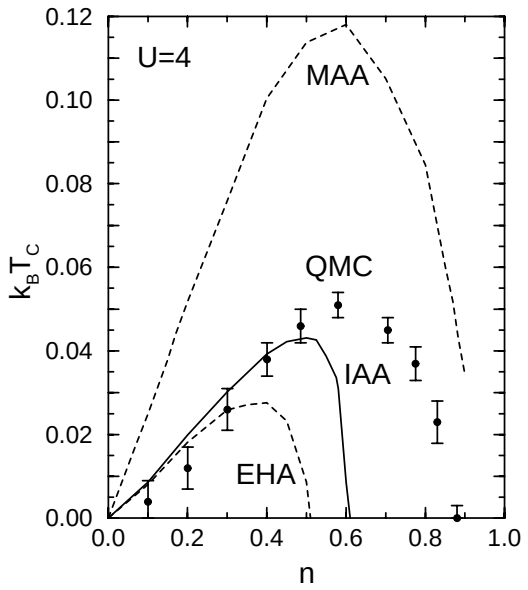

Fig. 7. Filling dependence of the Curie temperature at $U = 4$ within the MAA, EHA and IAA in comparison with the QMC result (error bars) by Ulmke [44].

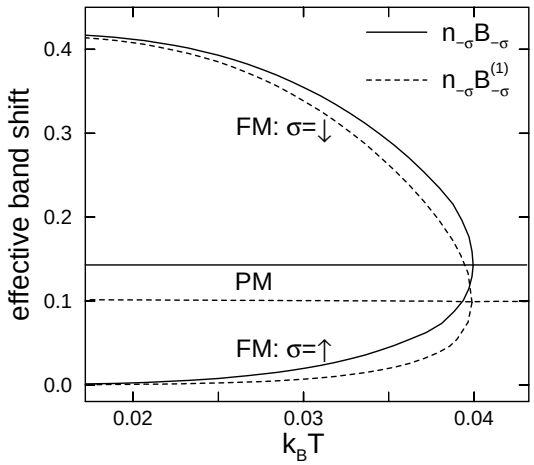

Fig. 8. Effective band shift $n_{-\sigma}B_{-\sigma}$ and Hartree-Fock value $n_{-\sigma}B^{(1)}_{-\sigma}$ calculated within the IAA as a function of temperature for the ferromagnetic (FM) and the paramagnetic phase (PM), $d = \infty$ fcc lattice, $U = 4$, $n = 0.4$.

there is a too high T_C within the MAA can be attributed to the fact that quasi-particle damping is underestimated compared with the IAA (*cf.* preceding subsection). Damping effects tend to reduce the density of states at the Fermi edge which according to Stoner's criterion implies a lower T_C [29]. The difference in the Curie temperatures between the EHA and IAA must result from the approximation $B_{-\sigma} \mapsto B^{(1)}_{-\sigma}$. The temperature dependence of the corresponding effective band shifts is shown in Figure 8 for $n = 0.4$. In the paramagnetic phase $n_{-\sigma}B_{-\sigma}$ and $n_{-\sigma}B^{(1)}_{-\sigma}$ are (almost) temperature independent. In the ferromagnetic phase below T_C there is a spin splitting of both quantities. As $T \mapsto 0$ the fully polarized state is reached, and $n_\downarrow = 0$ implies a vanishing effective band shift $n_\downarrow B_\downarrow = n_\downarrow B^{(1)}_\downarrow = 0$. On the other hand, for $T \mapsto 0$ we have $\Sigma_\uparrow(E) \mapsto 0$ which implies *via* equations (9, 26) that $n_\uparrow B_\uparrow - n_\uparrow B^{(1)}_\uparrow \mapsto 0$. Figure 8 shows that in both cases, $\sigma = \uparrow, \downarrow$, the difference $n_{-\sigma}B_{-\sigma} - n_{-\sigma}B^{(1)}_{-\sigma}$ increases with increasing T and is at its maximum for $T = T_C$, *i.e.* for the paramagnet. For the ferromagnet we can conclude that replacing $B_{-\sigma}$ by $B^{(1)}_{-\sigma}$ in the *self-consistent* solution for the self-energy, will result in small changes of the spin-dependent spectral density only. These are comparable to those discussed in the previous subsection for the paramagnet. More important, however, *within* the self-consistency cycle the effective band shift can have a strong influence on the magnetic aspects of the final solution. Therefore, using the Hartree-Fock approximation for $B_{-\sigma}$ may be insufficient to describe the magnetic properties of the system.

Analyzing the continued-fraction expansion of the Green function for $T = 0$, Uhrig [40] could obtain the exact boundary $U = U_N(n)$ above which the fully polarized state is stable against a single spin flip for the fcc-type lattice. Due to the divergence of the BDOS at the lower band edge, the Nagaoka state is locally stable even for low fillings $n \mapsto 0$, the (in-) stability line smoothly ends at $U_N(0) = 0$. To compare with these results, Figure 9 shows the filling-dependence of the magnetization for different U at a low temperature $T = 0.01$. At low fillings the system is paramagnetic. Above a critical filling $n_{c,1}(U)$ a non-zero magnetization is found which steeply increases with increasing n and (almost) reaches the saturation value $m = n$. Finally, for higher $n > n_{c,2}(U)$ ferromagnetism breaks down again. The higher critical filling $n_{c,2}(U)$ exhibits an unusual U dependence: it is at its maximum for $U = 2$ and decreases for larger $U > 2$. This is believed to be an artefact of the method; we expect the IAA to be able to yield reliable information up to $n \approx 0.5$ only. On the other hand, the U dependence of the lower critical filling is plausible: $n_{c,1}(U)$ monotonically decreases with increasing U. We have inspected the IAA result for $U = 1$ in more detail for lower temperatures. Even at $T = 0.001$ the system is not fully polarized for low fillings. We found it difficult to access still lower temperatures numerically. Extrapolating the temperature dependence of the magnetization to $T = 0$, however, we find our results to be consistent with a ferromagnetic phase extending to $n = 0^+$. For larger fillings extrapolation to $T = 0$ yields the value n_N up to which the system remains fully polarized. Figure 9 shows that the obtained fillings n_N for $U = 1.0, 1.5, 2.0$ are close to the results found by Uhrig [40]. For the larger values of U ($U > 2$) the IAA is not able reproduce $n_N(U)$, *e.g.* a partially polarized ground state for $U = 4$ and $n = 0.58$ is inconsistent with the results of reference [40] but is found in the IAA (see Fig. 6).

To estimate to which strength of the interaction U the IAA is a reliable approach, we have calculated the

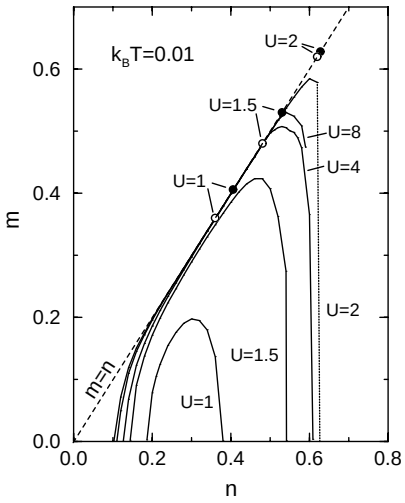

Fig. 9. Filling dependence of the magnetization at $k_BT = 0.01$ and different values of U. The lower critical filling $n_{c,1}(U)$, above which ferromagnetism occurs for $k_BT = 0.01$, decreases with increasing U. The open circles indicate the filling $n_N(U)$ below which the system remains fully polarized at $T = 0$: $n_N(1.0) = 0.36 \pm 0.03$, $n_N(1.5) = 0.48 \pm 0.02$, $n_N(2.0) = 0.62 \pm 0.02$ (errors due to the extrapolation to $T = 0$). For comparison the exact results for n_N by Uhrig [40] are also shown (filled circles).

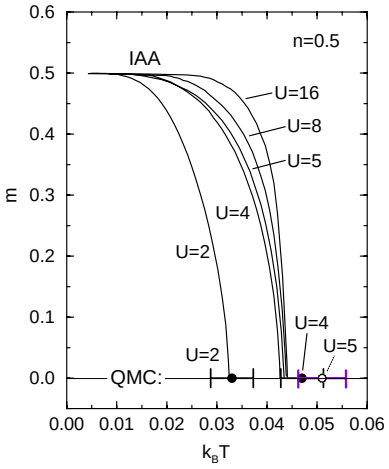

Fig. 10. Temperature dependence of the magnetization at $n = 0.5$ and different values of U. The QMC data for T_C at $U = 2, 4, 5$ are taken from the interpolation lines in Figure 2 of reference [44]; the bars indicate the typical (QMC) errors.

temperature-dependent magnetization for different U at the filling $n = 0.5$. The results are shown in Figure 10. For each U considered we observe ferromagnetic saturation for $T \mapsto 0$ and a second-order transition to the paramagnetic phase at the respective Curie temperature $T_C(U)$. As a function of U the Curie temperature is found to saturate with $T_C(U = \infty) \approx 0.044$. We also included the predictions of the QMC method for $T_C(U)$ in Figure 10. The

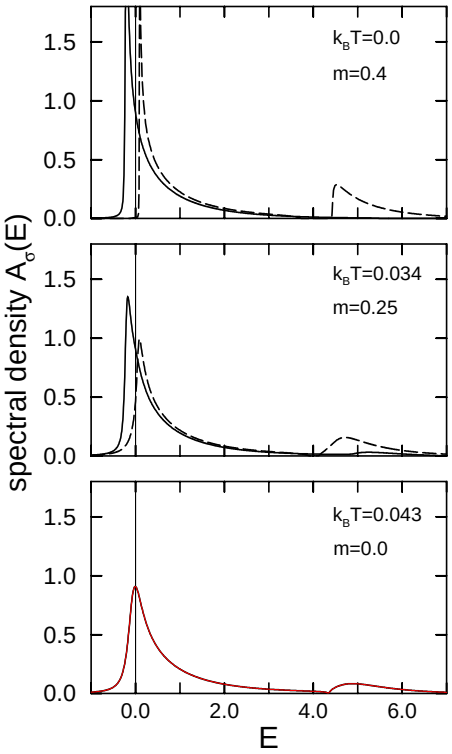

Fig. 11. Spin-dependent spectral density in the ferromagnetic phase for three different temperatures ($d = \infty$ fcc lattice, $U = 4$, $n = 0.4$). Solid line: majority spin ($\uparrow$). Dashed line: minority spin ($\downarrow$). $k_BT = 0.043$ corresponds to the Curie temperature.

data for $U = 2, 4, 5$ are taken from the values of the interpolation lines at $n = 0.5$ in Figure 2 of reference [44]. The error bars represent the respective *typical* error as has been estimated from the real data points and errors in the vicinity of $n = 0.5$. There is a convincing agreement between IAA and QMC for $U = 2$. At $U = 4$ the IAA result for T_C still falls into the error bounds, while a slightly too low T_C is predicted for $U = 5$. We conclude that for strong interaction U the IAA appears to be reasonable but less convincing compared with the low and intermediate U regime [47].

The temperature-dependence of the spin-resolved spectral densities is shown in Figure 11. We have taken $n = 0.4$ and $U = 4$ where the IAA should yield reliable results. For $T = 0$ the shape of the $\uparrow$ spectral density is given by the shape of the free BDOS (3) since the magnetization is saturated, $m = n$, and thus $\Sigma_\uparrow \equiv 0$. The square-root singularity at the lower band edge has been slightly smeared out for numerical reasons. We have checked that this does not affect the presented results for m, χ^{-1} and T_C. The $\downarrow$ spectral density is split into the lower and the upper Hubbard band, the energetic distance of which is roughly given by U. For $U = 4$ the result of Harris and Lange should apply. The energetic shift between the $\uparrow$ band and the lower $\downarrow$ Hubbard band (centers of gravity) is read off from Figure 11 to be $T_{1\downarrow} - T_{1\uparrow} \approx 0.40$. On the other hand, the calculated effective band shift for the $\downarrow$ band is $n_\uparrow B_\uparrow = 0.42$ (see also Fig. 8). This is consistent with

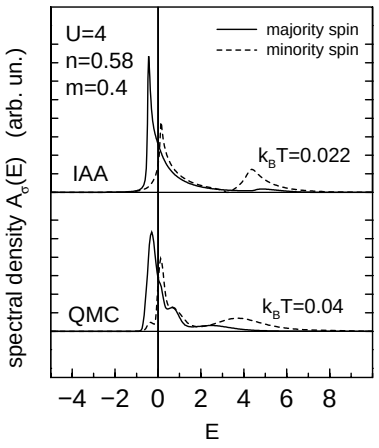

Fig. 12. Spin-dependent spectral density for $U = 4$ and $n = 0.58$. Comparison between the IAA result for $k_BT = 0.022$ and the QMC result from [44] for $k_BT = 0.04$. In both cases the magnetization is $m = 0.4$.

equation (12) which for the present case and averaged over $\mathbf{k}$ simplifies to $T_{1\downarrow} - T_{1\uparrow} = n_\uparrow B_\uparrow$.

With increasing temperature the upper Hubbard band in the $\uparrow$ spectral density arises. There is an exchange splitting between the $\uparrow$ and $\downarrow$ upper Hubbard bands being inverse to the splitting between their lower counterparts. For $T \mapsto T_C$ the spin splitting becomes gradually smaller. At the same time we observe a transfer of spectral weight between the two spin channels that speeds up the depolarization of the system. At $T = T_C$ both spectra have become identical. Compared with the $T = 0$ case, the singularity at the lower band edge has disappeared, and a strong broadening of the spectrum can be observed which is due to quasi-particle damping.

The qualitative behavior of the spectral density as a function of temperature, *i.e.* what concerns the spin-dependent centers of gravity, effective widths and spectral weights of the Hubbard bands, very well agrees with the results of Harris and Lange. This implies that the higher-order corrections in the t/U expansion that have been neglected in equation (12) can be considered to be small (for $U = 4$).

At the same interaction strength, but for higher filling there is one QMC result available for the spin-dependent spectral density in the ferromagnetic phase [44]. Unfortunately, the filling ($n = 0.58$) and the temperature ($T = 0.04$) where the QMC spectrum has been obtained, are not well suited for a one-to-one comparison between IAA and QMC since the Curie temperature predicted by the IAA is below $T = 0.04$ (see Fig. 6). We therefore try a comparison of the QMC spectrum with the IAA result at $T = 0.022$ where the magnetization is non-zero and equal to the magnetization found within QMC ($m = 0.4$). Figure 12 shows the resulting spin-dependent spectral densities. A quantitative agreement with the QMC spectrum cannot be expected: due to the temperature dependence of the effective band shift $n_{-\sigma}B_{-\sigma}$, the positions and weights of the Hubbard bands cannot be the same as those in QMC spectrum at a different temperature. Qualitatively, we notice that apart from the Hubbard bands there is an additional peak in the $\uparrow$ and the $\downarrow$ QMC spectrum at $E \approx 0.8$ and also a peak at $E \approx -0.4$ in the $\downarrow$ channel which is not seen in the IAA result. At zero energy we observe a weak shoulder in the $\uparrow$ QMC spectrum reminiscent of the Kondo resonance. A (much weaker) structure at $E = 0$ is also found by the IAA.

7 Conclusion

Exactly solvable limiting cases represent strong necessary conditions for any approximate solution of the Hubbard model. The central idea of the present paper has been to develop an analytical expression for the self-energy that is compatible with as much rigorous results as possible. From this point of view, the interpolating alloy-analogy-based approximation (IAA) can be considered as one of the best analytical approaches that are available for the Hubbard model in infinite dimensions.

It avoids the defects of the modified alloy analogy (MAA) [29] which is not able to recover Fermi-liquid properties in the weak-coupling regime, and it improves upon the Edwards-Hertz approximation (EHA) [25,27] which is at variance with the exact strong-coupling results of Harris and Lange. The IAA not only recovers the trivial $U = 0$ and the $t = 0$ limits but also the respective first non-trivial corrections: for small U it is exact up to order U^2 and can thus be regarded as a generalization of standard weak-coupling perturbation theory. For strong U it yields the correct positions and weights of the Hubbard bands which are exactly known from perturbation theory in t/U. Formally, the IAA is constructed by a proper combination of the MAA with the EHA: the general form of the ansatz for the self-energy it taken from the EHA, but following the concept of the MAA, the "atomic levels" and "concentrations" are determined by comparison with the first four exactly known moments of the spectral density. As a consequence, the coefficients of the high-energy expansion of the self-energy are exact up to order $1/E^2$. Furthermore, when applied to the Falicov-Kimball model, *i.e.* when suppressing the hopping of one spin species, the IAA reduces to the conventional alloy-analogy solution which has been shown to be exact in $d = \infty$ by Brandt and Mielsch.

The main disadvantage of the method consists in the fact that it cannot be motivated from a simple and physical concept. Inherently, its justification rests on its interpolating character only. In particular, the IAA is not conserving in the sense of Baym and Kadanoff. This must be taken into account when interpreting Fermi-surface and related properties. For the symmetric case of a paramagnet at half-filling the IAA simply reduces to the EHA which predicts the Mott transition but also a non-Fermi-liquid metallic phase. Within the EHA and similarly for the IAA, the latter turns out to be existing in a fairly extended region of the $T = 0$ phase diagram. On the other hand for $d = \infty$ there are no indications for non-Fermi-liquid behavior in combined studies with iterative

perturbation theory and quantum Monte-Carlo (QMC) simulations [8]. The non-Fermi-liquid metallic phase found in the IAA must be tightly connected with the alloy-analogy basis of the approximation and thus with the limit of the Falicov-Kimball model since it is known that in this limit the (mobile) electrons indeed do not form a Fermi liquid [7].

For an *a posteriori* test of the quality of the IAA, we have compared the results with numerically exact quantum Monte-Carlo data from Jarrell and Pruschke [38] as well as from Ulmke and Vollhardt *et al.* [43,44], with the results of Uhrig concerning the (in-) stability of the Nagaoka state [40] and with the results of the MAA and the EHA, mainly for the decisive moderate- to strong-coupling regime.

For the paramagnet on the hyper-cubic lattice, the differences between the EHA and IAA results are rather small, and judged from the QMC data, the IAA only slightly improves upon the MAA and EHA. At fillings close to half-filling the IAA fails to reproduce the Kondo-like quasi-particle peak in the spectrum, and an artificial ferromagnetic solution is found. Reliable results can only be expected for smaller n. Here, good overall agreement with QMC data is found regarding the spectral density as well as the static susceptibility.

Considerable improvement upon the MAA and the EHA is achieved for the description of spontaneous ferromagnetic order on a $d = \infty$ fcc-type lattice. For fillings up to quarter filling and for weak and moderate interaction strength U, the IAA is able to predict the magnetic properties and particularly the Curie temperatures very reliably. Also the results for strong interactions $U/t^* \leq 16$ at $n = 0.5$ seem to be still plausible. On the other hand, the approximation breaks down for fillings larger than $n \approx 0.5$. The MAA yields a clearly too high T_C which is due to an underestimation of quasi-particle damping. The EHA is as reliable as the IAA at low fillings where it predicts a Curie temperature consistent with the QMC result. However, for fillings larger than $n \approx 0.3$ the Curie temperatures are too low, and a paramagnetic ground state is found for $n > 0.51$ (at $U = 4$). Thus the EHA breaks down at a considerably lower filling compared with the IAA.

In our opinion this is due to the effect of a higher-order correlation function $B_{-\sigma}$ which is of special importance for several reasons: inclusion of $B_{-\sigma}$ is necessary to ensure the correct high-energy behavior of the theory as well as the correct moments of the spectral density (up to $m = 3$). This is the main condition to recover the exact strong-coupling results of Harris and Lange. For $U \mapsto \infty$ and in the ferromagnetic phase, the correlation function $B_{-\sigma}$ results in a *spin-dependent* shift $n_{-\sigma}B_{-\sigma}$ of the center of gravity of the lower Hubbard band. Thus the stability of ferromagnetic order is intimately related to the effective band shift. It is known that ferromagnetic order cannot be found at all or only under extreme circumstances within the Hubbard-I or the alloy-analogy solution where T_0 appears in place of $B_{-\sigma}$ in the high-energy expansion coefficients of the self-energy.

The apparent importance of the band shift for magnetic order provokes the question whether it is possible to construct analytical approaches that on the one hand are exact up to the $m = 3$ moment and on the other avoid the deficiencies of the IAA concerning its low-energy behavior. For example, up to now there is no *conserving* theory to our knowledge that correctly accounts for the $m = 3$ moment.

Support of this work by the Deutsche Forschungsgemeinschaft within the Sonderforschungsbereich 290 ("Metallische dünne Filme: Struktur, Magnetismus und elektronische Eigenschaften") is gratefully acknowledged.

References

1. J. Hubbard, Proc. R. Soc. Lond. A **276**, 238 (1963).
2. M.C. Gutzwiller, Phys. Rev. Lett. **10**, 159 (1963).
3. J. Kanamori, Prog. Theor. Phys. (Kyoto) **30**, 275 (1963).
4. E.H. Lieb, F.Y. Wu, Phys. Rev. Lett. **20**, 1445 (1968).
5. W. Metzner, D. Vollhardt, Phys. Rev. Lett. **62**, 324 (1989).
6. E. Müller-Hartmann, Z. Phys. B **74**, 507 (1989).
7. D. Vollhardt, in *Correlated Electron Systems*, edited by V.J. Emery (World Scientific, Singapore, 1993), p. 57.
8. A. Georges, G. Kotliar, W. Krauth, M.J. Rozenberg, Rev. Mod. Phys. **68**, 13 (1996).
9. M. Jarrell, Phys. Rev. Lett. **69**, 168 (1992).
10. M.J. Rozenberg, X.Y. Zhang, G. Kotliar, Phys. Rev. Lett. **69**, 1236 (1992).
11. A. Georges, W. Krauth, Phys. Rev. Lett. **69**, 1240 (1992).
12. M. Caffarel, W. Krauth, Phys. Rev. Lett. **72**, 1545 (1994).
13. Q. Si, M.J. Rozenberg, G. Kotliar, A.E. Ruckenstein, Phys. Rev. Lett. **72**, 2761 (1994).
14. H. Schweitzer, G. Czycholl, Z. Phys. B **83**, 93 (1991).
15. E. Halvorsen, G. Czycholl, J. Phys.: Condens. Matter **6**, 10331 (1994).
16. J.M. Luttinger, Phys. Rev. **119**, 1153 (1960).
17. A.B. Harris, R.V. Lange, Phys. Rev. **157**, 295 (1967).
18. H. Eskes, A.M. Oleś, M.B.J. Meinders, W. Stephan, Phys. Rev. B **50**, 17980 (1994).
19. M. Potthoff, T. Wegner, W. Nolting, Phys. Rev. B **55**, 16132 (1997).
20. L.M. Falicov, J.C. Kimball, Phys. Rev. Lett. **22**, 997 (1969).
21. U. Brandt, C. Mielsch, Z. Phys. B **75**, 365 (1989); *ibid.* **79**, 295 (1990); *ibid.* **82**, 37 (1991).
22. J. Hubbard, Proc. R. Soc. Lond. A **281**, 401 (1964).
23. V. Janiš, D. Vollhardt, Z. Phys. B **91**, 317 (1993).
24. V. Janiš, J. Mašek, D. Vollhardt, Z. Phys. B **91**, 325 (1993).
25. D.M. Edwards, J.A. Hertz, Physica B **163**, 527 (1990).
26. D.M. Edwards, J. Phys.: Condens. Matter **5**, 161 (1993).
27. S. Wermbter, G. Czycholl, J. Phys.: Condens. Matter **6**, 5439 (1994).
28. S. Wermbter, G. Czycholl, J. Phys.: Condens. Matter **7**, 7335 (1995).
29. T. Herrmann, W. Nolting, Phys. Rev. B **53**, 10579 (1996).

30. E. Müller-Hartmann, in: *Proc. V Symp. Phys. of Metals*, edited by E. Talik, J. Szade (Ustron-Jaszowiec, Poland, 1991), p. 22.
31. This differs from the choice of $t^* = t/\sqrt{2Z}$ for the hypercubic lattice. For the fcc lattice $t^* = t/\sqrt{Z}$ and $T_{\langle ij\rangle} > 0$ has been preferred here to be consistent with the results of Refs. [43,44].
32. W. Nolting, W. Borgieł, Phys. Rev. B **39**, 6962 (1989).
33. M. Potthoff, W. Nolting, J. Phys.: Condens. Matter **8**, 4937 (1996).
34. B. Velicky, S. Kirkpatrick, H. Ehrenreich, Phys. Rev. **175**, 747 (1968).
35. T. Herrmann, W. Nolting, J. Magn. Magn. Mat. **170**, 253 (1997).
36. E. Müller-Hartmann, Solid State Commun. **12**, 1269 (1973).
37. We define the moments $M^{(m)}_{\mathbf{k}\sigma} = \int E^m A_{\mathbf{k}\sigma}(E)dE/\hbar$ of the $\mathbf{k}$-resolved spectral density $A_{\mathbf{k}\sigma}(E)$. The moments can be calculated from $M^{(m)}_{\mathbf{k}\sigma} = \langle[\mathcal{L}^m c_{\mathbf{k}\sigma}, c^\dagger_{\mathbf{k}\sigma}]_+\rangle$ resulting in $M^{(m)}_{\mathbf{k}\sigma} = M^{(m)}_\sigma(\epsilon(\mathbf{k}))$. Interpreting the moments as the high-energy expansion coefficients of the $\mathbf{k}$-resolved Green function $G_{\mathbf{k}\sigma}(E) = \hbar/(E-(\epsilon(\mathbf{k})-\mu)-\Sigma_\sigma(E))$, leads to the same expansion coefficients $C^{(m)}_\sigma$ for the self-energy as given by equation (11).
38. M. Jarrell, T. Pruschke, Z. Phys. B **90**, 187 (1993).
39. P. Fazekas, B. Menge, E. Müller-Hartmann, Z. Phys. B **78**, 80 (1990).
40. G.S. Uhrig, Phys. Rev. Lett. **77**, 3629 (1996).
41. Y. Nagaoka, Phys. Rev. **147**, 392 (1966).
42. T. Obermeier, T. Pruschke, J. Keller, Phys. Rev. B **56**, 8479 (1997).
43. D. Vollhardt, N. Blümer, K. Held, M. Kollar, J. Schlipf, M. Ulmke, Z. Phys. B **103**, 283 (1997).
44. M. Ulmke, Euro. Phys. J. B **1**, 301 (1998).
45. J. Wahle, N. Blümer, J. Schlipf, K. Held, D. Vollhardt, cond-mat/9711242 (1997).
46. T. Hanisch, G.S. Uhrig, E. Müller-Hartmann, Phys. Rev. B **56**, 13960 (1997).
47. This also means that comparing with the NCA results of Obermeier *et al.* (Ref. [42]) for the partially polarized state on the hc lattice at very strong U near half-filling does not seem to be promising.